Removal of Heavy Metals from Domestic Wastewater using Beneficiated Kaolin Clay, Silver Oxide and Zinc Oxide Nanocomposite

F.O. Ogundipe[1*], M. Saidu[2], A.S. Abdulkareem[3], A.O Busari[2]

[1]Federal Ministry of Water Resources, Abuja, Nigeria
[2]Department of Civil Engineering, Federal University of Technology, Minna, Nigeria
[3]Department of Chemical Engineering, Federal University of Technology, Minna, Nigeria

ABSTRACT: This study describes the removal of total iron, cadmium, lead, copper, manganese, arsenic, mercury silver and zinc from domestic wastewater disposed of via sewers, using Beneficiated Kaolin Clay (BKC), BKC/Ag, BKC/ZnO and BKC/Ag/ZnO nanocomposite adsorbents produced by blending Silver Oxide (Ag) and Zinc Oxide (ZnO) nanoparticles with kaolin clay. High Resolution Transmission Electron Microscope (HRTEM) results showed that the produced adsorbents were polycrystalline in nature, while the interplanar spacing and average crystalline sizes are 1.775 – 4.712 nm and 26. 834 – 40.258 nm respectively, according to X-Ray Diffractometer (XRD) analysis. The Dispersive X – Ray Fluorescence (XRF) analysis indicated that SiO_2/Al_2O_3 ratios for BKC/Ag, BKC/ZnO and BKC/Ag/ZnO nanocomposites adsorbents were 1.5170, 1.4818 and 1.5231 respectively. Brunauer – Emmett – Teller (BET) analysis showed that the desorption average pore sizes fell in the mesopore widths of 13.8994 – 16.9233 nm and surface areas of 1.0545 - 14.5126 $m^2.g^{-1}$. The removal efficiencies of the produced adsorbents followed this trend: BKC/Ag/ZnO > BKC/Ag > BKC/ZnO > BKC. These adsorbents were excellent in the removal of total iron, cadmium, lead, copper, manganese, arsenic, mercury silver and zinc pollutants from domestic wastewater, and hence, recommended for large scale production.

KEYWORDS: Adsorption, Kaolin Clay, Heavy Metal removal, Domestic Wastewater, Nanocomposite

[Received March 26, 2023; Revised May 16, 2023; Accepted July 7, 2023] Print ISSN: 0189-9546 | Online ISSN: 2437-2110

I. INTRODUCTION

Waterbodies are imperative for human existence and the ability of rivers to support aquatic life and sustain other uses relies on some trace elements present in the waterbody. Manganese, zinc and copper when present in trace concentrations are necessary for physiology of living tissue. However, direct discharge of wastewater to rivers at heavy metals' concentrations above the permissible limits will have severe toxicological effects on humans' health, deteriorate water quality and aquatic ecosystem (NWQRL, 2020). Wastewater discharge, agricultural runoff and inadequate treatment of wastewater at household level, will continue to pollute water quality around the world. The use of heavy metals in the soaps and body creams manufacturing industries over the past few decades has seriously contributed to a rise in the flow of metallic compounds into household wastewater and has raised significant ecological and health threats to human beings (Syafiqa *et al*, 2021). The domestic wastewater investigated in this research work was collected via sewers that connected toilets, baths, showers, kitchen and sinks together. Domestic wastewater in Nigeria is in most cases discharged into the adjoining environment with water bodies being mostly affected (Okereke *et al*, 2016). Nigeria is the Africa's most populous nation with 36 states and Federal Capital Territory, with the estimated population of over 213 million (Worldometer, 2023). A wastewater polluted river is sometimes consumed by villagers living downstream, who have no other source of potable water. Consumption and the use of this polluted river by the villagers are led to disease outbreak such as cholera, diarrhoea and at extreme cases, loss of lives. Acute lead poisoning in Zamfara State, Nigeria in 2010 led to illness and deaths (Roadmap, 2022) of more than 400 children mostly under 5 years old (Lo *et al*, 2010) in Bukkuyum and Anka Local Government Areas (Galadima and Garba, 2012). Aside from this direct impact, mercury poisoning has been linked to fish consumption (Aguilar *et al*., 2009). Currently, there is a very rampant of kidney diseases in Maiduguri, Borno State, Nigeria which are suspected to be associated with consumption of mercury polluted water and food. Consumption of water with intolerable level of copper ions has also reportedly caused gastrointestinal disturbances, abdominal pains, nausea and vomiting (Aguilar *et al*., 2009). Aquatic lives are equally affected by the presence of heavy metal ions and organic molecules in wastewater (Edema, 2012).

In an effort to remove heavy metal contaminants from the wastewater, conventional treatment methods (Rajasulochana and Preethy, 2016; Grégorio and Eric, 2019), adsorption (Rakhi *et al*, 2016; Amandeep & Sangeeta, 2017; Dhaval & Painter, 2017) and Filtration (Fu and Wang, 2011) have been

*Corresponding author: ogundipefelixo@yahoo.com

doi: http://dx.doi.org/10.4314/njtd.v18i4.1651

used for wastewater treatment for a while, but not without drawbacks. Conventional wastewater treatment methods have high cost of labour, chemicals consumption and sludge handling problem (Chan *et al*, 2009). Complexity and membrane fouling are major drawbacks in the use of filtration method (Fu and Wang, 2011). The price of commercial adsorbent such as commercially available activated carbon is costly (Mohd *et al*, 2013) and difficult to regenerate due to rapid saturation and clogging (Grégorio and Eric, 2019).

Advances in nanoscale science and engineering suggest that many of the current problems involving water quality could be resolved by using nanocomposite (Berekaa, 2016), bioactive nanoparticles (Sukdeb *et al*, 2007; Thabet *et al*, 2010; Njagi *et al*, 2010; Vikas *et al*, 2013; Benakashani *et al*, 2016; Shittu and Ikebana, 2017), nanostructured catalytic membranes (Rui *et al*, 2013), nanocomposite (Abdullah *et al*, 2017), nanotubes, magnetic nanoparticles (Ming et al, 2012; Sulekha, 2016; Vikas et al, 2013), high surface area metal particle (Ralf *et al*, 2011; Sierra *et al*, 2018; Maity *et al*, 2018) with characteristic length scales of 9-10 nm (Haijiao *et al* 2016). As an environmentally friendly material, nanocomposite adsorbents could efficiently remove heavy metals (Ming *et al*, 2012), Chromium VI (Rui *et al*, 2013), enhance adsorption of lead ion (Yang *et al*, 2008) and use as antibacterial application (Getie S *et al*, 2017b; Haritha *et al*, 2011; Ying *et al*, 2017; Stoyanova *et al*, 2013). However, it was noticed that none of the research work reviewed, reported the blend of silver and zinc oxide nanoparticles on clay support from Kutigi, Niger State, to remove heavy metals from wastewater collected via household sewers. In view of the danger associated to discharge of domestic wastewater to waterbodies and in a bid to protect the environment from further pollution, this research work developed nanocomposite adsorbents from produced by blending Silver Oxide (Ag) and Zinc Oxide (ZnO) nanoparticles with kaolin clay to remove total iron, cadmium, lead, copper, manganese, arsenic, mercury silver and zinc from the domestic wastewater.

Kaolin clay, an aluminosilicate mineral (Yahaya *et al*, 2017; Kuranga *et al* 2018), is classified as potential solid mineral in Niger State, Nigeria (NBS, 2017). There is deposit of kaolin clay in 13 local government areas of the state namely, Agaie, Bida, Bosso, Edati, Gbako, Katcha, Lapai, Lavun, Mashegu, Mokwa, Paikoro, Shiroro and Wushishi (RMRDC, 2012). The kaolin clay minerals are widely utilized for agriculture, ceramics (Auta and Hameed, 2013), environmental applications (Murray, 2000), absorbents (Saikia *et al*, 2003; Bachiri *et al*, 2014) and wastewater treatment (Chun *et al*, 2013; Cheng *et al*, 2017), production of metakaolin (Kuranga *et al*, 2018; Wilson *et al*, 2017). Attention is on clay materials because of their sheet-like structures that provides high specific surface area (Dhaval & Painter, 2017; Sachin *et al*, 2013; Aroke and Onatola, 2016).

II. MATERIALS AND METHOD

Mangifera Indica Leaves for green synthesis of silver and zinc nanoparticles were collected from River Basin Estate, Tundun Fulani, Minna. The kaolin clay was collected from Kutigi, Nigeria, while the domestic wastewater collected via sewer that connected toilets, baths, showers, kitchen and sinks together. Analytical grade chemicals and reagents used in this research work are listed in Table 1.

A. Beneficiation of Kaolin Clay

200 g of raw kaolin clay lumps were put in 4 Litres Beakers with 4 Litres of distilled water added. This represents 5 % w/w kaolin clay slurry in distilled water. The Beaker was stirred for 1 hour using Heildolph RGL500 High viscosity stirrer at control speed of 40 revolutions per minute for adequate dispersion in distilled water. The resulting mixture was allowed to swell in distilled water for 22 hrs 57 mins as calculated by Stoke's Law using Eqn. 1.

$$u_s = \frac{g(\rho_p - \rho_w)d_p^2}{18\mu} \quad (1)$$

Where ρ_p = particle density, kg/m^3 (Kaolin clay particle = 1600 kg/m^3), μ = liquid viscosity, kg/m.s (distilled water = 8.90×10^{-4} Pa·s), ρ_w = density of water, kg/m^3 (997 kg/m^3), u_s= Particle settling velocity, m/s, d_p = diameter of particle (m), g = acceleration due to gravity, m/s^2 (9.81 m/s^2), t = Settling Time, R = particle size (radius) of clay, assumed to be spherical (1µm = 1 X 10^{-6}m), h = Settling Height of Fluid (12 cm = 0.12 m), The resultant slurries were thereafter dried in a laboratory oven at a temperature of 105 ^{o}C until the water is evaporated and the samples weight became constant. Acid activation was done by treating the beneficiated kaolin clay with 0.5 M of HCl to remove carbonate, washed by 10 % Hydrogen Peroxide (H_2O_2) to oxide organic matter (Bachiri *et al*, 2014) and NaCl to remove nutrients (Cheng *et al*, 2017). The residue from filtration was washed several times with distilled water and monitored until pH 7. The percentage yield (Y) of the beneficiated clay was calculated using Eqn. 2.

$$Y = \frac{Mass\ of\ Purified\ Kaolin\ Clay\ Produced}{Mass\ of\ Raw\ Kaolin\ Clay}\ x\ 100\% \quad (2)$$

Table 1: List of Reagents/Chemicals

S/N	Chemical/Reagents	Formula	% Purity	Manufacturer
1	Silver Nitrate	$AgNO_3$	99.5	BDH Chemicals Ltd., Poole, England
2	Deionised Distilled Water	DDW	0.5 µS/cm	FMWR – NWQRL Minna
3	Zinc Sulphate, (Heptahydrate),	$ZnSO_4.7H_2O$	99	LOBA Chemie, Mumbai, India
4	Zinc Chloride	ZnCl	99.5	J.T Baker Limited, Philipsburg USA
5	Ethanol	C_2H_5OH	96	EMD Millipore Corporation, Germany
6	Ammonium Hydroxide	NH_4OH	30-32	Tyuangdang Guanghua Chemical Factory Company Limited, China
7	Hydrogen Peroxide Solution	H_2O_2	30-32	BDH Chemicals Ltd., Poole, England

B. Green Syntheses of ZnO Nanoparticles

10 g of Zinc Sulphate Heptahydrate ($ZnSO_4.7H_2O$) powder was measured and put in 250 mL volumetric flask. DDW was added to 100 mL mark of the volumetric flask. The resultant mixture was stirred using a magnetic stirrer at 150 rpm for 30 minutes. 50 mL volume of the prepared concentration was collected and put in another 100 mL conical flask. The conical flask was put on the hot plate and temperature set to 80 ^oC. *Mangifera Indica* leave (Maity *et al*, 2018) extract (titrant) was put in a burette, ready for titration. The solution was titrated, while continuously stirred at 80 ^oC until the light-yellow colour was formed (Sierra *et al*, 2018; Daizy, 2010). The titration was stopped immediately colour change was observed (Manokari and Mahipal, 2016; Thirunavukkarasu *et al*, 2016). The stirring continued for 10 mins until a colloid was obtained. The solution consumed 4.9 mL of titrant. The resultant mixture was filtered and washed with DDW until the pH 7 was gotten. The precipitate was oven-dried at 105 ^oC for 6 hours and calcined in the furnace at 450 ^oC for 3 hours to obtain ZnO-NP. The ZnO-NP obtained was kept in a glass bottle for further characterisation and use.

C. Green Synthesis of Ag Nanoparticles

5 g of $AgNO_3$ (Thabet *et al*, 2010) powder was measured and synthesised as previously stated in (B) above. The conical flask was rapped with aluminium foil to avoid the photo degradation of silver during titration on the hot plate at 70 ^oC (Njagi *et al*, 2010; Shittu and Ikebana (2017; Vikas *et al*, 2013) The solution consumed 2.8 mL titrant. The dried Ag-NP obtained was kept in a glass bottle for further characterisation and use.

D. Production of Nanocomposite Adsorbents

The experimental procedures to produce BKC/Ag, BKC/ZnO, BKC/Ag/ZnO nanocomposites adsorbent for removal of heavy metal contaminants from domestic wastewater are as follows:

1) Synthesis of BKC/ZnO nanocomposites

1 g of $ZnSO_4.7H_2O$ powder was dissolved in 50 mL of DDW and stirred with magnetic stirrer for 30 min at 150 rpm. 50 mL of the prepared concentration was put in 100 mL conical flask.

The conical flask was put on the hot plate and titrated, while continuously stirred at 80 ^oC with *Mangifera Indica* leave extract until the light-yellow colour was formed. The solution consumed 2.6 mL of the titrant. To the suspension formed, 10 g of BKC was dispersed under vigorous stirring for 1 hour at 40 rpm. A homogeneous gel obtained was filtered by Whatman No. 1 filter paper and washed with DDW until the pH 7 was gotten. The gel was oven-dried at 105 ^oC for 6 hours and calcined in the furnace at 450 ^oC for 3 hours to obtain BKC/ZnO nanocomposite adsorbent.

2) Synthesis of BKC/Ag Nanocomposite

0.5 g of ANO_3 powder was dissolved in 50 mL of DDW and stirred for 30 min at 150 rpm. The prepared concentration was procesed as described in (1) above, but stirred at 70 ^oC.

3) Synthesis of BKC/Ag/ZnO Nanocomposite

0.5 g of $AgNO_3$ and 1 g of $ZnSO_4.7H_2O$ were dissolved in 50 mL of DDW and stirred to get a precursor. The prepared concentration was processed as described in (1) above to obtain BKC/Ag/ZnO nanocomposite adsorbent.

E. Characterisation

The structural changes in the beneficiated kaolin clay, Ag-NP, ZnO-NP, BKC/Ag, BKC/ZnO, BKC/Ag/ZnO nanocomposites adsorbents were analysed using the stated equipment in Table 2 below.

F. *Wastewater Analyses*

Wastewater were analysed to determine total iron, cadmium, lead, copper, manganese, arsenic, mercury silver and zinc. The selected heavy metals were analysed using Atomic Absorption Spectrometer (AAS) and Metalyser HM1000/5000 in line with 21st Edition of American Public Health Association (APHA, 2017) Standard Methods for Examination of Water and Wastewater.

G. *Adsorption Capacity*

The adsorption capacity of BKC, BKC/ZnO, BKC/Ag and BKC/Ag/ZnO to remove the selected heavy metals from the wastewater was tested using both Langmuir isotherms and Freundlich models. The effect of contact time, dosage and temperature were investigated at 10 - 60 mins, 5 – 30 g and 30 – 80 ^oC respectively.

Table 2: Characterisation of Ag/ZnO Nanoparticles, BKC/Ag, BKC/ZnO, BKC/Ag/ZnO Nanocomposites Adsorbents

S/N	Test Equipment and Model	Uses	Location
1	X-Ray Diffractometer (XRD), Emma 0141, GCB SCIENTIFIC EQUIPMENT	Determination of mineral phases and compounds in materials. Study of crystal structure of the mineral phases and compounds in materials	University of South Africa (UNISA), Johannesburg, South Africa
2	Dispersive X – Ray Fluorescence (XRF) Machine, EDXRF-3600B, OXFORD INSTRUMENT	Chemical analyses of materials	University of South Africa (UNISA), Johannesburg, South Africa
3	HRTEM, TECNAI G2, FEI Netherlands	Determination of Microstructure and particle size of materials	University of South Africa (UNISA), Johannesburg, South Africa
4	BET Nitrogen Absorption Analyser, TriStar II 3020, MICROMETRICS, USA	Determination of Pore sizes, Pore Volumes and Surface Areas	University of South Africa (UNISA), Johannesburg, South Africa
5	UV – Spectrometer, UV – 1800 SHMADZU, Japan	Determination of purity and concentration of a solution	Centre for Genetic Engineering and Biotechnology, FUT Minna

1) Langmuir isotherm

The rate change of concentration due to adsorption equals to the rate of concentration due to desorption as expressed in Eqn. 3.

$$\frac{Ce}{q_e} = \frac{1}{Q_o b} + \frac{Ce}{Qo} \quad (3)$$

Where Ce = Equilibrium concentration (mg/l), q_e = Amount adsorbed at equilibrium time (mg/g), Q_o = Langmuir constants derived from the slope, b = Langmuir constants derived from the intercept, The values of the Langmuir constants were calculated from the intercept and slope of the plot of $\frac{Ce}{q_e}$ versus Ce. The dimensionless separation factor expressed on favourable adsorption nature was calculated from Eqn. 4.

$$\boldsymbol{R_L} = \frac{\mathbf{1}}{(\mathbf{1} + \boldsymbol{bC_i})} \quad (4)$$

Where C_i = Initial concentration of the wastewater (mg/l), b = Langmuir constant (l/mg), R_L= indicate the type of isotherm as shown in Table 3.

Table 3: Isotherm Type

R_L Value	Type of Isotherm
$R_L > 1$	Unfavourable
$R_L = 1$	Linear
$R_L < 1$	Favourable
$R_L = 0$	Irreversible

2) Freundlich isotherm

Freundlich isotherm (Ikhazuangbe *et al*, 2017) is expressed as shown in Eqn. 5:

$$K_f C_e{}^{\frac{1}{n}} \quad (5)$$

However, the linearized Freundlich adsorption isotherm can be expressed as shown in Eqn. 6.

$$Log\ q_e = Log\ K_f + \frac{1}{n}\ Log\ C_e \quad (6)$$

Where C_e = Equilibrium concentration, q_e = Adsorption capacity at equilibrium stage, K_f and n = Freundlich constants which incorporates all factors affecting the adsorption process (adsorption capacity and intensity). Values of K_f and n were obtained from the intercept and slope of a plot of adsorption capacity (q_e) against equilibrium concentration (C_e). Both parameters K_f and n affect the adsorption isotherm. The larger the K_f and n values, the higher the adsorption capacity (Ikhazuangbe *et al*, 2017). When the value of n is greater than unity (1< n < 10) that means adsorption process is favourable (Bashir *et al*, 2013).

3) Thermodynamic studies

The thermodynamic parameters of the adsorption process were determined from the experimental data obtained at various temperatures using Eqns. 7 - 10 (Bashir *et al*, 2013; Ikhazuangbe *et al*, 2017; Al-Kadhi, 2019).

$$\Delta G = -RT ln K_d \quad (7)$$

$$K_d = \frac{q_e}{C_e} \quad (8)$$

$$ln K_d = \frac{\Delta So}{R} - \frac{\Delta Ho}{RT} \quad (9)$$

$$\Delta Go = \Delta Ho - T\Delta So \quad (10)$$

Where Kd = Distribution coefficient for the adsorption, q_e = Amount of contaminants adsorbed on the adsorbent per litre of wastewater at equilibrium, Ce = Equilibrium concentration (mg/L) of the contaminants in wastewater, T = Absolute temperature, R = Gas constant, ΔGo = Gibbs free energy change (kj/mol), ΔHo = Enthalpy change (kj/mol), ΔSo = Entropy change (J/K).

III. RESULTS AND DISCUSSION

A. Characterisation Results

1) XRD analyses

The XRD results for raw kaolin clay, BKC, Ag -NP, ZnO-NP, BKC/Ag, BKC/ZnO and BKC/Ag/ZnO were presented in Table 4. The raw and beneficiated kaolin clay displayed the existence of four crystalline phases of kaolinite – $Al(Si_2O_5)(OH)_4$, kaolinite 1Md – $AlSi_2O_5(OH)_4$, quartz – SiO_2 and muscovite – $Kal_2\ (Si_3Al)O_{10}(OH)_2$. The BKC/Ag nanocomposite adsorbent displayed four phases of kaolinite, quartz, muscovite and silver – 3s. XRD results of BKC/ZnO showed four phases of kaolinite, quartz, muscovite and zinc sulphate hydrate. XRD results of BKC/Ag/ZnO nanocomposite adsorbents displayed five phases which were kaolinite, quartz, muscovite, silver – 3c and zinc sulphate hydrate as presented in Table 4.

The broad peaks formation of XRD pattern showed that the raw kaolin clay, beneficiated kaolin, ZnO nanoparticles, BKC/Ag, BKC/ZnO and BKC/Ag/ZnO were polycrystalline while Ag nanoparticles were monocrystalline in nature. The Interplanar spacing and average crystalline sizes obtained as shown in Table 5 ranged from 1.775 nm – 4.712 nm and 26.834 nm - 40.258 nm respectively, at Scherrer's constant of 0.94 and wavelength (λ) of 1.5406 Å. The XRD results confirmed that nanoparticles and nanocomposites adsorbents have been successfully produced in this research work.

2) XRF analyses

The XRF analysis was further carried out on the obtained Ag-NP, ZnO-NP, BKC, BKC/Ag, BKC/ZnO and BKC/Ag/ZnO as shown in Table 6. The SiO_2/Al_2O_3 ratios of BKC/Ag, BKC/ZnO and BKC/Ag/ZnO nanocomposites adsorbents ware 1.5170, 1.4818 and 1.5231 respectively. The SiO_2/Al_2O_3 ratio, a function of the mineral phase present in BKC/Ag, BKC/ZnO and BKC/Ag/ZnO nanocomposites, indicated that a purer kaolinite has been produced when compared with the raw kaolin clay ratio of 1.54. The closer the SiO_2/Al_2O_3 ratio to unity the purer the kaolin. Loss on ignition (LOI) for BKC/Ag, BKC/ZnO and BKC/Ag/ZnO nanocomposites adsorbents was found to be 9.61%, 16.31% and 12.37 % respectively. The loss of silicate and the gain of alumina in the nanocomposite adsorbents could be attributed to the purification and treatment method employed for the beneficiation of the kaolin clay. The high LOI for the produced nanocomposite adsorbents may be attributed to the dehydroxylation reaction in the kaolin mineral. Loss on ignition for ZnO-NP, Ag-NP, BKC/Ag, BKC/ZnO and BKC/Ag/ZnO are 52.13%, 1.1%, 9.61%, 16.31%, 12.37% respectively. High LOI is an indication of potential normal porosity in the intended adsorbent for treatment of domestic wastewater as shown in Table 6.

Table 4: XRD Phase Identification of ZnO-NP, BKC, BKC/Ag, BKC/ZnO and BKC/Ag/ZnO

Phases	Formula	Raw Clay (%)	Ag-NP	ZnO-NP	BKC	BKC/Ag	BKC/ZnO	BKC/Ag/ZnO
Kaolinite	$Al(Si_2O_5)(OH)_4$	14.10	-	-	28.52	47.01	35.56	51.27
Kaolinite 1Md	$AlSi_2O_5(OH)_4$	15.04	-	-	19.01	-		
Quartz	SiO_2	66.41	-	-	46.85	38.23	53.38	41.69
Muscovite	$Kal_2(Si_3Al)O_{10}(OH)_2$	4.45	-	-	5.62	0.82	3.16	0.90
Silver – 3C	Syn – Ag	-	100	-	-	13.93	-	2.34
Zinc Sulphate Hydrate	ZnSO4 6H2O	-	-	-	-		7.90	3.80
Zinkosite, syn (NR)	$ZnSO_4$	-	-	24.74	-	-	-	-
Zinkosite	$ZnSO_4$	-	-	24.74	-	-	-	-
Gunnigile, syn	$ZNSO_4$ H_20	-	-	36.08	-	-	-	-
Zinc Oxide Sulphate	$Zn_3O(SO_4)_2$	-	-	8.25	-	-	-	-
Zinc Hydroxide	$Zn(OH)_2$	-	-	4.12	-	-	-	-
Zinc Hydrogen Sulphate	$Zn(HSO_4)_2$	-	-	2.06	-	-	-	-

Table 5: Crystallite Size of Ag-NP, ZnO-NP, BKC, BKC/Ag, BKC/ZnO and BKC/Ag/ZnO

Diffraction Angle, 2θ	d- spacing, (nm)	Crystallite Size, D, (nm)
Raw Kaolin	3.499	40.258
BKC	3.532	28.114
Ag Nanoparticles	1.775	30.629
ZnO Nanoparticles	3.435	32.038
BKC/Ag	3.818	25.574
BKC/ZnO	4.712	35.692
BKC/Ag/ZnO	3.887	26.934

bright spots and rings of the SAED patterns suggested the Ag-NP is monocrystalline in nature. SAED resolution pattern are consistent with the XRD and XRF results of Ag-NP as earlier stated in this study.

The crystal structure of ZnO-NP was analysed by HRTEM to know the crystal pattern at the scales approaching a single atom as presented in Plate IV (a – b). The SAED pattern in Plate IV (c) showed faded circles which suggested that the ZnO-NP is polycrystalline in nature.

Table 6: Mineralogy composition of Ag-NP, ZnO-NP, BKC, BKC/Ag, BKC/ZnO and BKC/Ag/ZnO

Compound	Raw Kaolin Clay (%)	Beneficiated Kaolin Clay	ZnO Nanoparticles	Ag Nanoparticles	BKC/Ag	BKC/ZnO	BKC/Ag/ZnO
Fe_2O_3 %	1.23	1.24	0.01	0.00	1.00	1.04	0.97
MnO %	0.00	0.00	0.00	0.00	0.00	0.01	0.00
Cr_2O_3 %	0.02	0.02	0.01	0.00	0.03	0.03	0.02
V_2O_5 %	0.00	0.00	0.00	0.00	0.03	0.03	0.02
TiO_2 %	1.69	1.75	0.05	0.01	1.61	1.69	1.58
CaO %	0.33	0.02	0.18	0.02	0.00	0.09	0.05
K_2O %	0.61	0.63	0.42	0.01	0.56	0.53	0.54
P_2O_5 %	0.07	0.05	0.04	0.00	0.05	0.04	0.03
SiO_2 %	52.64	48.55	0.00	0.00	45.80	44.13	46.21
Al_2O_3 %	34.18	35.95	0.02	0.00	30.19	29.78	30.34
MgO %	0.23	0.03	0.06	0.00	0.00	0.00	0.00
Na_2O %	0.11	0.14	9.21	0.02	0.18	1.16	0.40
LOI %	8.90	11.62	52.13	51.10	9.61	16.31	12.37
Total	100	100	62.15	53.56	89.10	94.82	92.55
SiO_2/Al_2O_3 Ratio	1.54	1.35	0.000	0.000	1.517	1.4818	1.5231

3) HRTEM analyses

The crystal patterns of the raw kaolin clay are presented in Plates I (a – b). The crystallinity of the kaolin clay was examined using Selected Area Electron Diffraction (SAED) pattern as shown in Plates I (c). The bright spots and rings of the SAED pattern suggested that the raw kaolin clay, is polycrystalline in nature.

HRTEM images in Plate II (a – b) showed the structure of the BKC with kaolinite particles of varying sizes arranged in face-to-face patterns. The crystal structure in Plate II (c) showed bright rings of SAED patterns which are polycrystalline, with each ring depicted diffraction pattern of BKC particles.

The crystallinity of Ag-NP was examined using SAED pattern and the results are presented in Plate III (a - c). The

The heavy dark colour images in V (a - b) indicated the presence of silver atoms and impregnation of Ag-NP on BKC, while the grey colour indicated crystal of different sizes. The bright spots and rings of the SAED pattern in Plate V (c) suggested that the BKC/Ag nanocomposite adsorbent is polycrystalline. The HRTEM images and SAED resolution pattern obtained were consistent with the results of XRD and XRF characterization in this study.

The heavy dark colour images in VI (a - b) indicated the presence of zinc atoms and impregnation of ZnO-NP on BKC as previously described in plate V. The bright spots and rings of the SAED pattern suggested that the nanocomposite adsorbent produced is polycrystalline in nature.

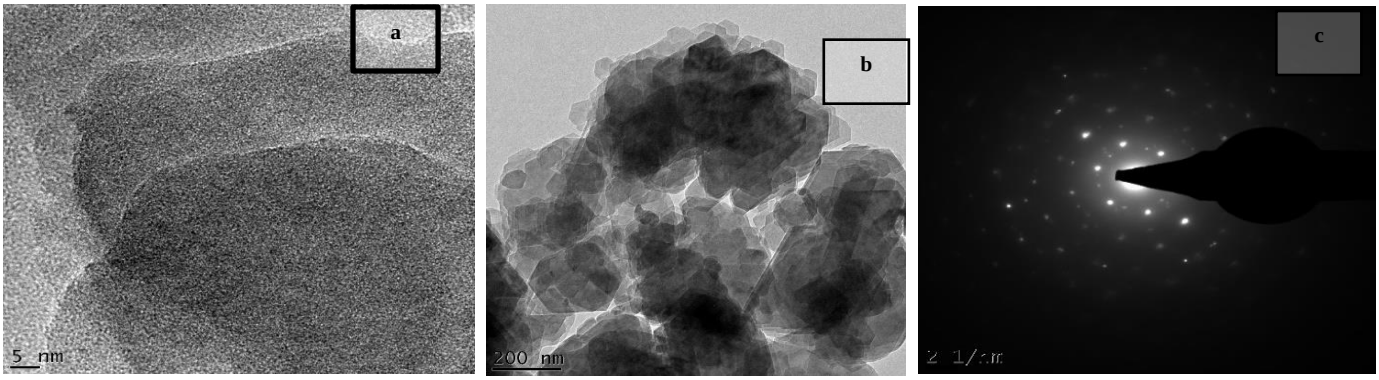

Plate I: HRTEM (a – b) and SAED (c) Images of Raw Kaolin Clay

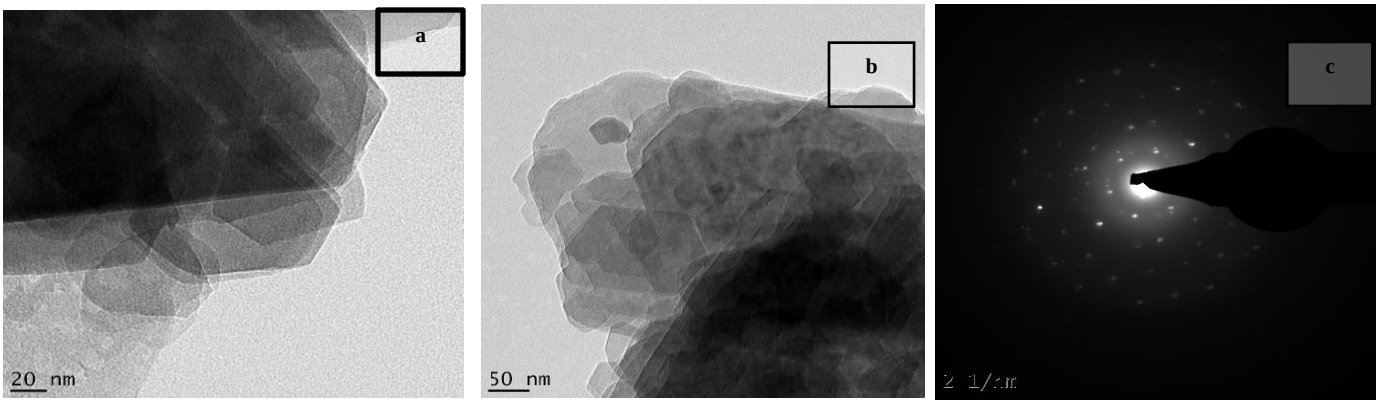

Plate II: HRTEM (a – b) and SAED (c) Images of Beneficiated Kaolin Clay

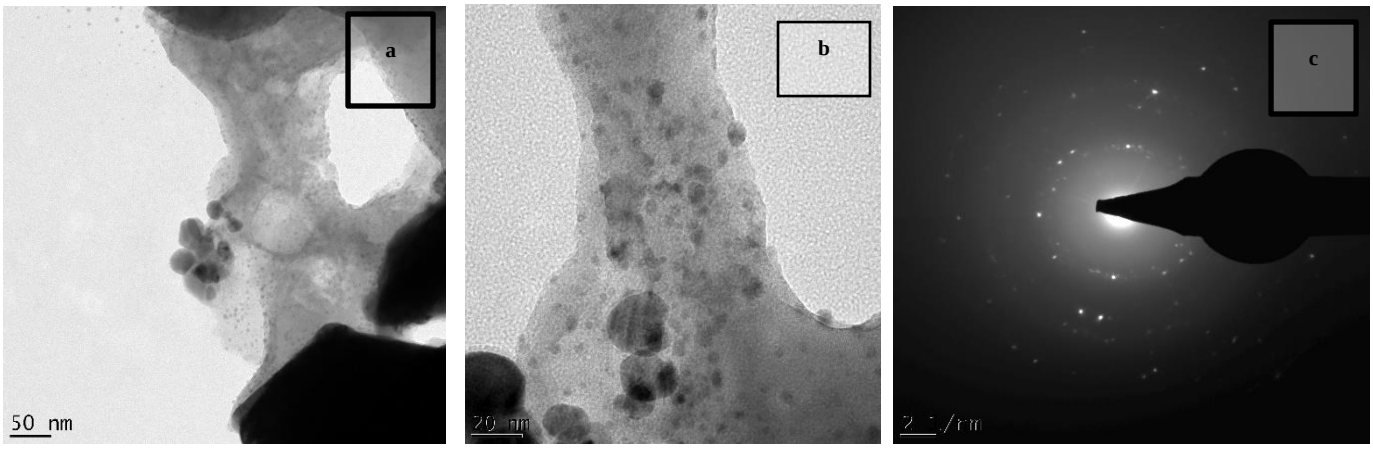

Plate III: HRTEM (a – b) and SAED (c) Images of Ag Nanoparticles

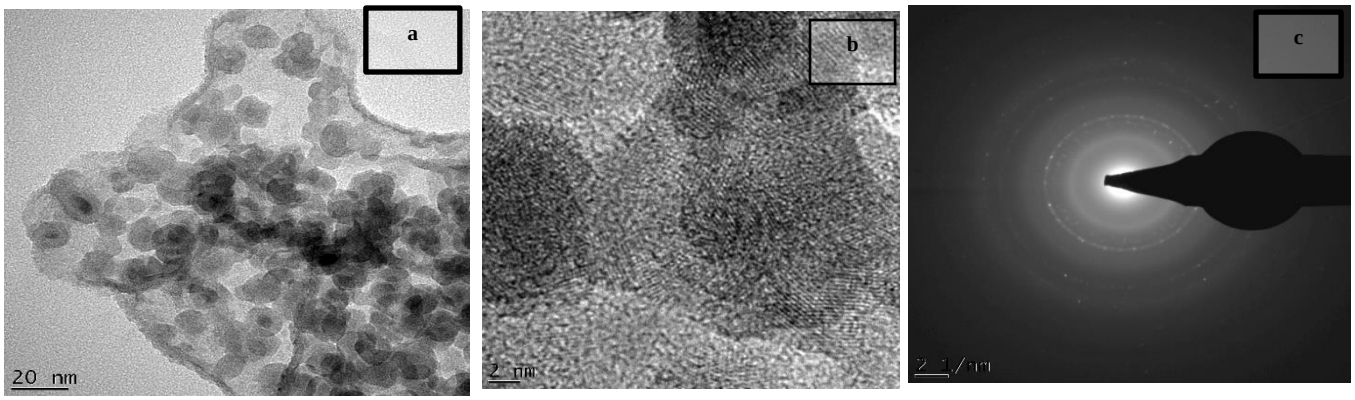

Plate IV: HRTEM (a – b) and SAED (c) Images of ZnO Nanoparticles

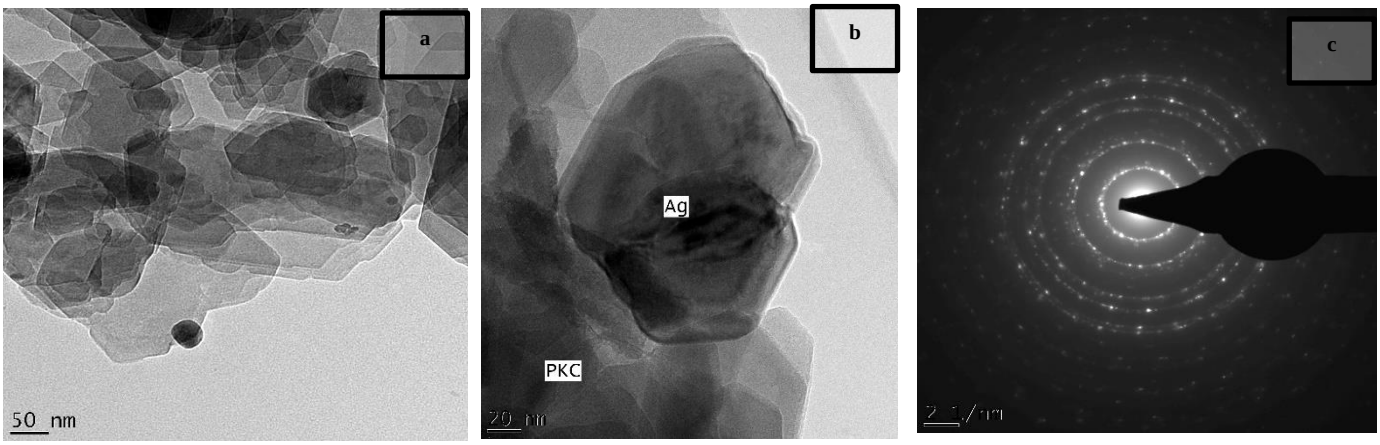

Plate V: HRTEM (a – b) and SAED (c) Images of BKC/Ag Nanocomposite Adsorbent

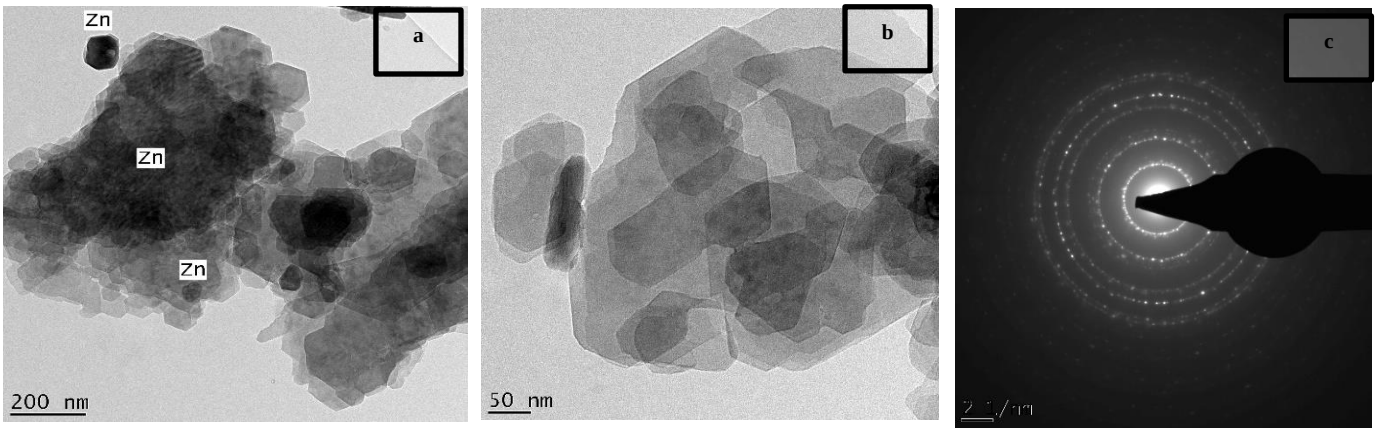

Plate VI: HRTEM (a – b) and SAED (c) Images of BKC/ZnO Nanocomposite Adsorbents

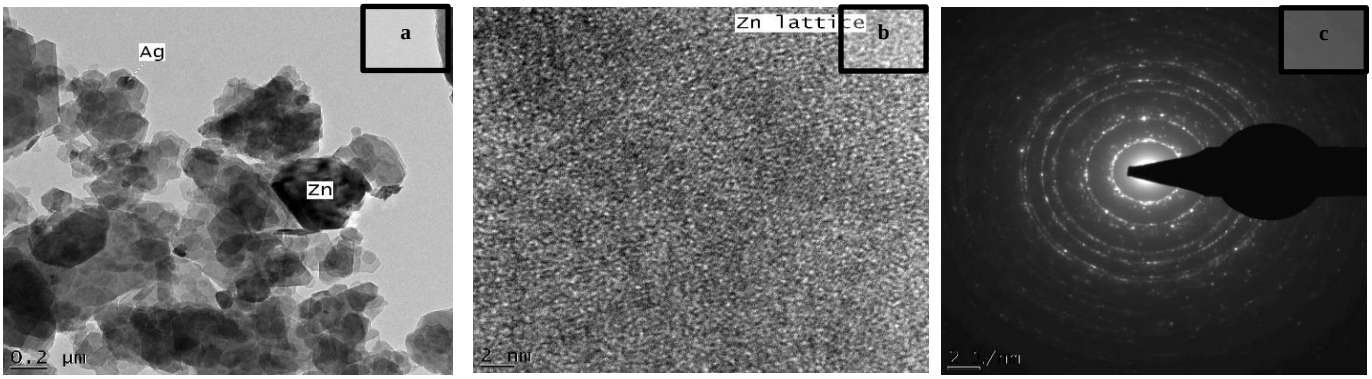

Plate VII: HRTEM (a – e) and SAED (f) Images of BKC/Ag/ZnO Nanocomposite Adsorbent

HRTEM images in Plate VII (a – b) clearly showed the impregnation of Ag-np and ZnO-np on BKC. The heavy dark colour images in Plate VII (c) indicated the presence of zinc and silver atoms, while the light or grey colour indicated crystal of different sizes. The HRTEM images and SAED resolution pattern obtained were consistent with the earlier results of XRD and XRF characterisation.

4) BET analyses

The BET analyses results in Table 7 showed that the desorption average pore diameters of BKC, BKC/Ag, BKC/ZnO and BKC/Ag/ZnO fell in the mesopore widths of 1.0422 - 13.8994 nm and surface areas of 1.0545 $\mathbf{m^2.g^{-1}}$ - 14.5126 $\mathbf{m^2.g^{-1}}$. The higher the surface area, the larger its adsorptive capacity. BKC/Ag/ZnO came out with the largest surface area.

B. Domestic Wastewater Analyses

The initial concentrations of total iron, lead, copper, manganese, arsenic, mercury silver and zinc in the domestic wastewater were determined and the results compared with National Environmental Standards Regulations and Enforcements Agency (NESREA, 2011) as presented in Table 8.

Table 7: Surface Area, Pore Size and Volume BKC, BKC/Ag, BKC/ZnO and BKC/Ag/ZnO Nanocomposite Adsorbents

Nanoparticles	Surface Area ($m^2.g^{-1}$)	Pores Volume (cm^3/g)	Pore Diameters (nm)	Pore Size (nm)
ZnO-NP	1.1045	0.000319	1.1555	16.8893
Ag-NP	1.0545	0.000269	1.1057	15.9899
BKC	14.5126	0.055738	13.8994	13.8994
BKC/Ag	11.9222	0.046930	1.1319	13.9066
BKC/ZnO	12.8245	0.053012	1.0422	14.6784
BKC/Ag//ZnO	12.8278	0.063671	1.0524	16.9233

Table 8: Domestic Wastewater Quality Analysis

Parameters	Units	Wastewater	NESREA (2011)
Total Iron	mg/L	0.83	0.5
Lead	mg/L	0.14	0.1
Copper	mg/L	0.05	0.01
Manganese	mg/L	0.25	-
Arsenic	mg/L	0.22	0.05
Mercury	mg/L	0.11	0.0005
Silver	mg/L	0.02	-
Zinc	mg/L	2.46	0.2

C. *Adsorption Studies*

1) Effect of contact time

The effect of contact time on the adsorption of selected heavy metals onto BKC, BKC/ZnO, BKC/Ag and BKC/Ag/ZnO nanocomposites adsorbents was studied at contact time of 10, 20, 30, 40, 50 and 60 mins using an adsorbent dosage of 25 g/100 mL of wastewater at a temperature of 29.5 ^oC and pH of 6.9. It was observed that an increase in the fraction of total iron, lead, copper, manganese, arsenic, mercury silver and zinc adsorbed occurred with corresponding increase in the contact time for the produced nanocomposite adsorbents as presented in Table 9. Rapid adsorption rates were obtained between the contact time of 10 – 40 mins. On reaching the equilibrium adsorption, the rate of adsorption equals the rate of desorption; therefore, the slow uptake and the slight or no decrease in heavy metal contaminant removal with further increase in contact time might be due to saturation of the surface area of the adsorbent with pollutants.

2) Effect of dosage

The effects of adsorbent dosage when treated with BKC, BKC/ZnO, BKC/Ag and BKC/Ag/ZnO nanocomposites adsorbents to remove the selected heavy metals from wastewater was studied at adsorbent dosages of 5 – 30 g, constant pH of 6.9, temperature of 29.4 ^oC and contact time fixed at 30 mins. The higher the adsorbent dosages used in the treatment, the higher the removal efficiencies of the pollutants from the wastewater. The observed trend in terms of total iron, lead, copper, manganese, arsenic, mercury silver and zinc removal were BKC/Ag/ZnO > BKC/Ag > BKC/ZnO > BKC as shown in Table 10. This is because of an increase in the availability of the active binding exchangeable sites and large surface areas of the adsorbents (Abukhadra and Mohamed, 2019).

3) Effect of temperatures

The effect of temperatures on the adsorption of iron, lead, copper, manganese, arsenic, mercury silver and zinc onto BKC, BKC/ZnO, BKC/Ag and BKC/Ag/ZnO nanocomposites adsorbents was studied at temperature of 30, 40, 50, 60, 70 and 80 ^oC using an adsorbent dosage of 25 g/100 ml of wastewater at pH of 6.9. The increase in temperature from 30^oC- 80^oC for the nanocomposite adsorbents gradually increased heavy metal adsorption. Slow uptake of pollutants was observed from 70 - 80 ^oC for nanocomposite adsorbent as presented in Table 11. The slow uptake and the slight or no increase in concentration removal with further increase in temperature might be due to saturation of the surface area of the adsorbent with pollutants.

D. Adsorption Isotherm

1) Langmuir isotherms

The Langmuir isotherms displayed a linear relationship between Ce and $\frac{Ce}{q_e}$ for all the tested parameters when treated with BKC, BKC/ZnO, BKC/Ag and BKC/Ag/ZnO nanocomposite adsorbents. The plot exhibits linearity and good correlation coefficient. Table 12 showed that the values of R^2 were very close to unit, showing a strong agreement with the Langmuir isotherm.

2) Freundlich adsorption isotherm

From the plot of adsorption capacity (q_e) against equilibrium concentration (C_e) for the removal of iron, lead, copper, manganese, arsenic, mercury silver and zinc in wastewater, the model showed the multilayer adsorption patterns and the fitting to the heterosporous nature of BKC, BKC/ZnO, BKC/Ag and BKC/Ag/ZnO nanocomposite adsorbents. It was evident that the linear correlation coefficients (R^2) were all greater than 0.90 as shown in Table 13. This showed that the experimental data moderately fit Freundlich adsorption isotherm. When the value of n is greater than unity ($1< n < 10$), the adsorption process is favourable.

E. Enthalpy (ΔH), Gibb's Free Energy (ΔG) and Entropy (ΔS) of Adsorption

The values of enthalpy change (ΔH^o) and entropy change (ΔS^o) were obtained from the slope and intercept of ln K_d versus 1/T plots. The values of ΔH^o and ΔS^o were found to be positive as presented in Table 14. The positive values of ΔH^o showed that the adsorption processes of the nanocomposite adsorbents were endothermic in nature. The negative values of ΔG^o indicated the adsorption of total iron, cadmium, lead, copper, manganese, arsenic, mercury silver and zinc pollutants onto the nanocomposite adsorbents, is spontaneous and exothermic over the study range of temperatures (Abbas *et al.*, 2020).

Table 9: Effect of Contact Time

Adsorbents	**Wastewater (mg/L)**	***Effect of contact time on total iron removal (mg/L)***					
		10 Mins	20 Mins	30 Mins	40 Mins	50 Mins	60 Mins
BKC	0.830	0.490	0.343	0.3087	0.123	0.139	0.139
BKC/ZnO	0.830	0.390	0.273	0.2457	0.098	0.034	0.034
BKC/Ag	0.830	0.380	0.266	0.2394	0.096	0.034	0.034
BKC/Ag/ZnO	0.830	0.350	0.245	0.2205	0.088	0.026	0.026
		Effect of contact time on lead removal (mg/L)					
BKC	0.140	0.120	0.084	0.076	0.030	0.009	0.009
BKC/ZnO	0.140	0.110	0.079	0.071	0.028	0.009	0.009
BKC/Ag	0.140	0.110	0.081	0.073	0.029	0.009	0.009
BKC/Ag/ZnO	0.140	0.090	0.063	0.057	0.023	0.007	0.007
		Effect of contact time on copper removal (mg/L)					
BKC	0.050	0.040	0.032	0.0259	0.010	0.008	0.008
BKC/Zn	0.050	0.040	0.029	0.0257	0.010	0.002	0.002
BKC/Ag	0.050	0.040	0.028	0.0252	0.010	0.002	0.002
BKC/Ag/Zn	0.050	0.030	0.021	0.0189	0.008	0.002	0.002
Adsorbents		*Effect of contact time on manganese removal, (mg/L)*					
BKC	0.250	0.190	0.133	0.1197	0.048	0.010	0.010
BKC/ZnO	0.250	0.170	0.119	0.1071	0.043	0.009	0.009
BKC/Ag	0.250	0.170	0.119	0.1071	0.043	0.009	0.009
BKC/Ag/ZnO	0.250	0.150	0.105	0.0945	0.038	0.008	0.008
		Effect of contact time on arsenic removal, (mg/L)					
BKC	0.220	0.095	0.0665	0.05985	0.024	0.020	0.020
BKC/ZnO	0.220	0.085	0.0595	0.05355	0.021	0.020	0.020
BKC/Ag	0.220	0.088	0.0616	0.05544	0.022	0.020	0.020
BKC/Ag/ZnO	0.220	0.082	0.0574	0.05166	0.021	0.020	0.020
		Effect of contact time on mercury removal, (mg/L)					
BK	0.110	0.092	0.0644	0.05796	0.023	0.018	0.018
BKC/Zn	0.110	0.075	0.0525	0.04725	0.019	0.018	0.018
BKC/Ag	0.110	0.073	0.0511	0.04599	0.018	0.018	0.018
BKC/Ag/ZnO	0.110	0.071	0.0497	0.04473	0.018	0.018	0.018
		Effect of contact time on silver removal, (mg/L)					
BKC, mg/L	0.02	0.012	0.0084	0.00756	0.003	0.003	0.003
BKC/ZnO	0.02	0.012	0.0084	0.00756	0.003	0.003	0.003
BKC/Ag	0.02	0.013	0.0091	0.00819	0.003	0.003	0.003
BKC/Ag/ZnO	0.02	0.012	0.0084	0.00756	0.003	0.003	0.003
		Effect of contact time on zinc removal, (mg/L)					
BKC	2.46	0.971	0.6797	0.61173	0.245	0.219	0.219
BKC/ZnO	2.46	0.994	0.6958	0.62622	0.250	0.219	0.219
BKC/Ag	2.46	0.959	0.6713	0.60417	0.242	0.219	0.219
BKC/Ag/Zn	2.46	0.87	0.609	0.54810	0.219	0.219	0.219

IV. CONCLUSION

Nanocomposite adsorbents were successfully produced and characterised. The efficacy of the adsorbents produced in the removal of total iron, cadmium, lead, copper, manganese, arsenic, mercury silver and zinc from domestic wastewater followed this trend: BKC/Ag/ZnO > BKC/Ag > BKC/ZnO > BKC. Both the Langmuir and Freundlich isotherms models were favourable, thus provided the good fits for predicting the adsorption of the selected heavy metals. ΔH^o and ΔS^o were positive which showed that the adsorptions processes were endothermic in nature The nanocomposite adsorbents produced is therefore recommended for use in the treatment of domestic wastewater.

AUTHOR CONTRIBUTIONS

M. Saidu: Supervision and Reviewing. **F.O. Ogundipe:** Conceptualisation and Writing. **A.S**. **Abdulkareem**: Supervision Reviewing and Editing. **A.O**. **Busari**: Supervision.

ACKNOWLEDGEMENT

OriginLab Corporation, Northampton, USA: Provision of Student version of OriginPro 2021b (trial) data and analysis software. Federal Ministry of Water Resources Abuja, Nigeria: Free access to National Water Quality Reference Laboratory Minna. Nanotech Research Group, Federal University of Technology, Minna: Interfacing and liaising with the University of South Africa to to characterize the Raw Kaolin Clay, BKC, BKC/AgO, BKC/ZnO and BKC/AgO/ZnO nanocomposite adsorbents.

Table 10: Effect of Dosage

Adsorbents	**Wastewater (mg/L)**	***Effect of adsorbents dosage on total iron removal (mg/L)***					
		5g	10g	15g	20g	25g	30g
BKC	0.830	0.730	0.511	0.4599	0.184	0.139	0.139
BKC/ZnO	0.830	0.710	0.497	0.4473	0.179	0.063	0.063
BKC/Ag	0.830	0.713	0.4991	0.44919	0.180	0.063	0.063
BKC/Ag/ZnO	0.830	0.690	0.483	0.4347	0.174	0.052	0.052
		Effect of adsorbents dosage on lead removal (mg/L)					
BKC	0.140	0.125	0.088	0.079	0.032	0.009	0.009
BKC/ZnO	0.140	0.122	0.085	0.077	0.031	0.009	0.009
BKC/Ag	0.140	0.123	0.086	0.077	0.031	0.009	0.009
BKC/Ag/ZnO	0.140	0.111	0.078	0.070	0.028	0.008	0.008
		Effect of adsorbents dosage on copper removal (mg/L)					
BKC	0.050	0.048	0.0336	0.03024	0.012	0.008	0.008
BKC/Zn	0.050	0.047	0.0329	0.02961	0.012	0.002	0.002
BKC/Ag	0.050	0.047	0.0329	0.02961	0.012	0.002	0.002
BKC/Ag/Zn	0.050	0.045	0.0315	0.02835	0.011	0.002	0.002
		Effect of adsorbents dosage on manganese removal, (mg/L)					
BKC	0.250	0.238	0.1666	0.14994	0.060	0.012	0.012
BKC/ZnO	0.250	0.230	0.161	0.1449	0.058	0.012	0.012
BKC/Ag	0.250	0.228	0.1596	0.14364	0.057	0.011	0.011
BKC/Ag/ZnO	0.250	0.225	0.1575	0.14175	0.057	0.011	0.011
		Effect of adsorbents dosage on arsenic removal, (mg/L)					
BKC	0.220	0.215	0.1505	0.13545	0.054	0.020	0.020
BKC/ZnO	0.220	0.2	0.14	0.126	0.050	0.020	0.020
BKC/Ag	0.220	0.199	0.1393	0.12537	0.050	0.020	0.020
BKC/Ag/ZnO	0.220	0.17	0.119	0.1071	0.043	0.020	0.020
		Effect of adsorbents dosage on mercury removal, (mg/L)					
BK	0.110	0.101	0.0707	0.06363	0.025	0.018	0.018
BKC/Zn	0.110	0.1000	0.0700	0.063	0.025	0.018	0.018
BKC/Ag	0.110	0.1000	0.0700	0.063	0.025	0.018	0.018
BKC/Ag/ZnO	0.110	0.099	0.0693	0.06237	0.025	0.018	0.018
		Effect of adsorbents dosage on silver removal, (mg/L)					
BKC, mg/L	0.02	0.02	0.014	0.0126	0.005	0.003	0.003
BKC/ZnO	0.02	0.017	0.0119	0.01071	0.004	0.003	0.003
BKC/Ag	0.02	0.017	0.0116	0.0104	0.004	0.003	0.003
BKC/Ag/ZnO	0.02	0.016	0.0112	0.01008	0.004	0.003	0.003
		Effect of adsorbents dosage on zinc removal, (mg/L)					
BKC	2.46	2.05	1.435	1.2915	0.517	0.219	0.219
BKC/ZnO	2.46	1.96	1.372	1.2348	0.494	0.219	0.219
BKC/Ag	2.46	1.94	1.358	1.2222	0.489	0.219	0.219
BKC/Ag/Zn	2.46	1.87	1.309	1.1781	0.471	0.219	0.219

Table 11: Effect of Temperature

Adsorbents	**Wastewater (mg/L)**	**Effect of temperature on total iron removal (mg/L)**					
		30 ºC	40 ºC	50 ºC	60 ºC	70 ºC	80 ºC
BKC	0.830	0.490	0.441	0.3969	0.218	0.206	0.115
BKC/ZnO	0.830	0.390	0.234	0.2106	0.063	0.019	0.019
BKC/Ag	0.830	0.380	0.228	0.2052	0.062	0.018	0.018
BKC/Ag/ZnO	0.830	0.350	0.210	0.189	0.057	0.017	0.017
		Effect of temperature on lead removal (mg/L)					
BKC	0.140	0.040	0.036	0.0324	0.018	0.017	0.009
BKC/ZnO	0.140	0.040	0.024	0.0216	0.006	0.002	0.002
BKC/Ag	0.140	0.040	0.024	0.0216	0.006	0.002	0.002
BKC/Ag/ZnO	0.140	0.030	0.018	0.0162	0.005	0.001	0.001
		Effect of Temperature on copper removal (mg/L)					
BKC	0.050	0.040	0.036	0.0324	0.018	0.017	0.009
BKC/Zn	0.050	0.040	0.024	0.0216	0.006	0.002	0.002
BKC/Ag	0.050	0.040	0.024	0.0216	0.006	0.002	0.002
BKC/Ag/Zn	0.050	0.030	0.018	0.0162	0.005	0.001	0.001
		Effect of temperature on manganese removal, (mg/L)					
BKC	0.250	0.190	0.171	0.1539	0.085	0.080	0.045
BKC/ZnO	0.250	0.170	0.102	0.0918	0.028	0.008	0.008
BKC/Ag	0.250	0.170	0.102	0.0918	0.028	0.008	0.008
BKC/Ag/ZnO	0.250	0.150	0.090	0.081	0.024	0.007	0.007
		Effect of Temperature on arsenic removal, (mg/L)					
BKC	0.220	0.095	0.0855	0.077	0.042	0.040	0.022
BKC/ZnO	0.220	0.085	0.051	0.0459	0.014	0.004	0.004
BKC/Ag	0.220	0.088	0.0528	0.0475	0.014	0.004	0.004
BKC/Ag/ZnO	0.220	0.082	0.049	0.0443	0.013	0.004	0.004
		Effect of temperature on mercury removal, (mg/L)					
BK	0.110	0.092	0.0828	0.0745	0.041	0.039	0.022
BKC/Zn	0.110	0.075	0.045	0.0405	0.012	0.004	0.004
BKC/Ag	0.110	0.073	0.0438	0.0394	0.012	0.004	0.004
BKC/Ag/ZnO	0.110	0.071	0.043	0.0383	0.012	0.003	0.003
		Effect of temperature on silver removal, (mg/L)					
BKC, mg/L	0.02	0.012	0.0108	0.0097	0.005	0.005	0.003
BKC/ZnO	0.02	0.012	0.0072	0.0065	0.002	0.001	0.001
BKC/Ag	0.02	0.013	0.0078	0.007	0.002	0.001	0.001
BKC/Ag/ZnO	0.02	0.012	0.007	0.0065	0.002	0.001	0.001
		Effect of temperature on zinc removal, (mg/L)					
BKC	2.46	0.971	0.8739	0.7865	0.433	0.409	0.228
BKC/ZnO	2.46	0.994	0.5964	0.5368	0.161	0.048	0.048
BKC/Ag	2.46	0.959	0.5754	0.5179	0.155	0.047	0.047
BKC/Ag/Zn	2.46	0.87	0.522	0.4698	0.141	0.042	0.042

Table 12: Langmuir Adsorption Isotherm

Parameters	Sample	Intercept = 1/Qob	Slope = 1/Qo	Qo	b	R_L	R^2
Total Iron	BKC	0.0122	0.2754	3.631082	22.57377	0.050668	0.9934
	BKC/Ag	0.005	0.1702	5.875441	34.04	0.034184	0.9882
	BKC/ZnO	0.0089	0.0521	19.19386	5.853933	0.170684	0.9672
	BKC/Ag/ZnO	0.0042	0.1479	6.761325	35.21429	0.033082	0.9965
Lead	BKC	0.0071	1.1212	0.891902	157.9155	0.043275	0.9787
	BKC/Ag	0.0073	0.9596	1.042101	131.4521	0.051538	0.9822
	BKC/ZnO	0.0071	0.9635	1.037883	135.7042	0.050004	0.9631
	BKC/Ag/ZnO	0.0067	0.9205	1.086366	137.3881	0.049421	0.9952
Copper	BKC	0.016	2.0667	0.483863	129.1688	0.134076	0.9369
	BKC/Ag	0.0106	79.47	0.012583	7497.17	0.002661	0.9941
	BKC/ZnO	0.0119	1.2395	0.806777	104.1597	0.161083	0.9767
	BKC/Ag/ZnO	0.0086	1.7186	0.581869	199.8372	0.090976	0.991
Manganese	BKC	0.004	0.6663	1.500825	166.575	0.023450	0.9815
	BKC/Ag	0.0042	0.5856	1.70765	139.4286	0.027888	0.9804
	BKC/ZnO	0.0045	0.5536	1.806358	123.0222	0.031491	0.9691
	BKC/Ag/ZnO	0.004	0.5564	1.797268	139.1	0.027952	0.9809
Arsenic	BKC	0.202	3.3463	0.298838	16.56584	0.215309	0.9311
	BKC/Ag	0.1976	1.6134	0.619809	8.16498	0.357616	0.9501
	BKC/ZnO	0.1807	1.7948	0.557165	9.932485	0.313957	0.9719
	BKC/Ag/ZnO	0.0977	1.7992	0.555803	18.41556	0.197964	0.9638
Mercury	BKC	0.1395	3.2893	0.304016	23.57921	0.278264	0.9453
	BKC/Ag	0.1175	3.8017	0.26304	32.35489	0.219345	0.9828
	BKC/ZnO	0.1084	4.0524	0.246767	37.38376	0.19561	0.9748
	BKC/Ag/ZnO	0.0724	4.7933	0.208625	66.2058	0.120734	0.9841
Silver	BKC	0.3093	18.319	0.054588	59.22729	0.457761	0.9453
	BKC/Ag	0.2787	21.549	0.046406	77.3197	0.392712	0.9616
	BKC/ZnO	0.2712	21.99	0.045475	81.08407	0.381435	0.9683
	BKC/Ag/ZnO	0.2619	22.469	0.044506	85.79229	0.368209	0.9697
Zinc	BKC	0.2320	0.2493	4.011231	1.074569	0.274466	0.9912
	BKC/Ag	0.1888	0.2956	3.38295	1.565678	0.206119	0.9816
	BKC/ZnO	0.2037	0.3023	3.307972	1.484045	0.215019	0.9765
	BKC/Ag/ZnO	0.1632	0.3255	3.072197	1.994485	0.169307	0.9843

Table 13: Freundlich Isotherm Constants for BKC, BKC/Ag, BKC/ZnO and BKC/Ag/ZnO

Parameter	Sample	Intercept = log K	Slope = 1/n	n	K	R^2
Total Iron	BKC	0.7723	0.3789	2.639219	5.919704	0.9924
	BKC/Ag	1.3575	0.5808	1.721763	22.77718	0.9985
	BKC/ZnO	1.7951	0.8777	1.139341	62.38785	0.9986
	BKC/Ag/ZnO	1.5296	0.6394	1.563966	33.85322	0.995
Lead	BKC	1.0632	0.6455	1.549187	11.56645	0.9703
	BKC/Ag	1.2293	0.7055	1.417434	16.95509	0.9787
	BKC/ZnO	1.2498	0.7106	1.407261	17.77461	0.9678
	BKC/Ag/ZnO	1.2695	0.7083	1.411831	18.59945	0.9942
Copper	BKC	1.0592	0.7682	1.301744	11.46041	0.9962
	BKC/Ag	2.0419	1.0654	0.938615	110.1286	0.9936
	BKC/ZnO	1.4556	0.8586	1.164687	28.5496	0.9999
	BKC/Ag/ZnO	1.3846	0.8015	1.247661	24.24376	0.9995
Manganese	BKC	1.0796	0.5500	1.818182	12.01158	0.9989
	BKC/Ag	1.2264	0.6057	1.650982	16.84225	0.9982
	BKC/ZnO	1.2689	0.6273	1.594134	18.57377	0.9969
	BKC/Ag/ZnO	1.2983	0.6265	1.596169	19.87467	0.9999
Arsenic	BKC	-0.2105	0.5283	1.892864	0.615886	0.8866
	BKC/Ag	0.1336	0.6904	1.448436	1.360191	0.9658
	BKC/ZnO	0.0862	0.6459	1.548227	1.219551	0.9692
	BKC/Ag/ZnO	0.0236	0.5672	1.763047	1.055845	0.9929
Mercury	BKC	0.0269	0.6217	1.608493	1.063898	0.9397
	BKC/Ag	0.0758	0.5485	1.823154	1.190694	0.9568
	BKC/ZnO	0.1099	0.5245	1.906578	1.287953	0.9199
	BKC/Ag/ZnO	0.3071	0.3792	2.637131	2.02815	0.9727
Silver	BKC	-0.2209	0.7376	1.355748	0.601312	0.9821
	BKC/Ag	-0.3401	0.6796	1.471454	0.456983	0.982
	BKC/ZnO	-0.3438	0.676	1.47929	0.453106	0.9788
	BKC/Ag/ZnO	-0.4022	0.6461	1.547748	0.396096	0.987
Zinc	BKC	0.3006	0.5611	1.782214	1.998021	0.9725
	BKC/Ag	0.2973	0.491	2.03666	1.982896	0.9404
	BKC/ZnO	0.2781	0.5	2.00000	1.897143	0.9396

Table 14: Thermodynamic Parameters

Parameters	**Adsorbents**	**Intercept = $\Delta S^o/R$**	**Slope = - $\Delta H^o/R$**	**R^2**	**R (Jmol^{-1} K^{-1})**	**ΔS^o (J/K)**	**ΔH^o ((kj/mol)**	**ΔG^o (kj/mol)**					
Total Iron	**BKC**	**16.465**	**-4738**	**0.9366**	**8.3145**	**137**	**39394**	303	313	323	333	343	353
								-2086	-3455	-4824	-6193	-7562	-8931
	BKC/ZnO	29.58	-8560	0.9396	8.3145	246	71172	-3349	-5808	-8267	-10727	-13186	-15646
	BKC/Ag	29.476	-8515	0.939	8.3145	245	70798	-3461	-5912	-8362	-10813	-13264	-15715
	BKC/Ag/ZnO	29.185	-8386	0.9373	8.3145	243	69725	-3800	-6227	-8653	-11080	-13507	-15933
Lead	BKC	22.167	-6873.9	0.9643	8.3145	184	57153	1308	-535	-2378	-4221	-6064	-7908
	BKC/ZnO	34.078	-10285	0.9545	8.3145	283	85515	-338	-3171	-6005	-8838	-11672	-14505
	BKC/Ag	34.074	-10285	0.9545	8.3145	283	85515	-328	-3161	-5994	-8827	-11660	-14493
	BKC/Ag/ZnO	31.502	-9331	0.9482	8.3145	262	77583	-1780	-4399	-7019	-9638	-12257	-14876
Copper	BKC	20.284	-6192.9	0.9571	8.3145	169	51491	390	-1297	-2984	-4670	-6357	-8043
	BKC/ZnO	34.426	-10410	0.9549	8.3145	286	86554	-175	-3038	-5900	-8762	-11625	-14487
	BKC/Ag	34.426	-10410	0.9549	8.3145	286	86554	-175	-3038	-5900	-8762	-11625	-14487
	BKC/Ag/ZnO	30.938	-9113.5	0.9461	8.3145	257	75774	-2168	-4740	-7312	-9885	-12457	-15029
Manganese	BKC	19.275	-5821	0.9524	8.3145	160	48399	-161	-1763	-3366	-4969	-6571	-8174
	BKC/ZnO	32.054	-9540.7	0.9501	8.3145	267	79326	-1427	-4092	-6758	-9423	-12088	-14753
	BKC/Ag	32.054	-9540.7	0.9501	8.3145	267	79326	-1427	-4092	-6758	-9423	-12088	-14753
	BKC/Ag/ZnO	30.938	-9113	0.9461	8.3145	257	75770	-2172	-4744	-7317	-9889	-12461	-15034
Arsenic	BKC	14.985	-4095.8	0.9256	8.3145	125	34055	-3697	-4943	-6189	-7435	-8681	-9927
	BKC/ZnO	28.928	-8267	0.9357	8.3145	241	68736	-4142	-6547	-8953	-11358	-13763	-16168
	BKC/Ag	29.024	-8312.3	0.9363	8.3145	241	69113	-4007	-6421	-8834	-11247	-13660	-16073
	BKC/Ag/ZnO	28.836	-8222.6	0.9351	8.3145	240	68367	-4280	-6677	-9075	-11472	-13870	-16267
Mercury	BKC	21.406	-6600.2	0.9616	8.3145	178	54877	949	-830	-2610	-4390	-6170	-7950
	BKC/ZnO	32.082	-9551.5	0.9502	8.3145	267	79416	-1408	-4075	-6743	-9410	-12078	-14745
	BKC/Ag	31.803	-9446.1	0.9493	8.3145	264	78540	-1581	-4226	-6870	-9514	-12159	-14803
	BKC/Ag/ZnO	31.539	-9345.6	0.9484	8.3145	262	77704	-1752	-4374	-6997	-9619	-12241	-14864
Silver	BKC	16.582	-4785.9	0.9374	8.3145	138	39792	-1983	-3361	-4740	-6119	-7497	-8876
	BKC/ZnO	30.938	-9113	0.9461	8.3145	257	75770	-2172	-4744	-7317	-9889	-12461	-15034
	BKC/Ag	31.603	-9370.3	0.9486	8.3145	263	77909	-1708	-4336	-6963	-9591	-12218	-14846
	BKC/Ag/ZnO	30.938	-9113.5	0.9461	8.3145	257	75774	-2168	-4740	-7312	-9885	-12457	-15029
Zinc	BKC	14.74	-3974.6	0.9233	8.3145	123	33047	-4088	-5313	-6539	-7764	-8990	-10215
	BKC/ZnO	29.054	-8326	0.9365	8.3145	242	69227	-3969	-6385	-8800	-11216	-13632	-16048
	BKC/Ag	28.952	-8278.4	0.9359	8.3145	241	68831	-4108	-6515	-8922	-11329	-13737	-16144
	BKC/Ag/ZnO	28.713	-8161.9	0.9342	8.3145	239	67862	-4474	-6862	-9249	-11636	-14024	-16411

REFERENCES

Abbas, M.; Harrache, Z. and Trari, M. (2020). Mass-transfer processes in the adsorption of crystal violet by activated carbon derived from pomegranate peels: Kinetics and thermodynamic studies. *Journal of Engineered Fibers and Fabrics, 15, 155892502091984.* doi:10.1177/1558925020919847, pp 1-11.

Abdullah, A. A.; B.A. Mansor; M.A. Naif; M.K. Halimah; M.Z. Hussein and A.I. Nor. (2017). Preparation of Zeolite/Zinc Oxide Nanocomposites for toxic metals removal from water. *Elsevier Results in Physics* 7 (2017). http://dx.doi.org/10.1016/j.rinp.2017.01.036, pp723–731.

Abukhadra, M.R. and Mohamed, A.S. (2019). Adsorption removal of safranin dye contaminants from water using various types of natural zeolite. *Silicon*, 11(3), pp 1635-1647.

Aguilar F.; U.R Charrondiere; B. Dusemund; P. Galtier; J. Gilbert; D,M. Gott; S. Grilli; R. Guertler; G.E.N. Kass; J. Koenig; C. Lambré; J.C. Larsen; J.C. Leblanc; A. Mortensen; I. Parent-Massin; I.M.C.M. Pratt; I. Rietjens; P. Stankovic; T. Tobback; R.A. Verguieva and D. Woutersen. (2009). Copper (II) oxide as a source of copper added for nutritional purposes to food supplements. *The EFSA Journal* 1089, 1-15.

Al-Kadhi, N. S. (2019). The kinetic and thermodynamic study of the adsorption Lissamine Green B dye by micro-particle of wild plants from aqueous solutions. *The Egyptian Journal of Aquatic Research*. doi:10.1016/j.ejar.2019.05.004.

Amandeep K. and Sangeeta S. (2017). Removal of Heavy Metals from Wastewater by using various adsorbents - A Review. *Indian Journal of Science and Technology*, Vol 10(34), DOI: 10.17485/ijst/2017/v10i34/117269.

APHA (2017). *Standard methods for Examination of Water and Wastewater*. APHA, AWWA, WEF. 23rd Edition, Published by E and FN SPON, Washington D.C.

Aroke, U. O. and Onatola-Morakinyo S. (2016). Comparative Sorption of Diatomic Oxyanions onto HDTMA-Br Modified Kaolinite Clay. *International Journal of Engineering and Science* Vol.6, Issue 7 (August 2016), ISSN (e): 2278-4721, ISSN (p):2319-6483, www.researchinventy.com, pp 01-09.

Auta M. and Hameed B.H. (2013). Acid modified local clay beads as effective low-cost adsorbent for dynamic adsorption of methylene blue. *Journal of Industrial and Engineering Chemistry*, 1153–1161, http://dx.doi.org/10.1016/j.jiec.2012.12.012.

Bachiri, E.M.; E. Akichouh; H. Miz; S. Salhi and A. Tahani. (2014). Adsorptions desorption and kinetics studies of Methylene Blue Dye on Na-bentonite from Aqueous Solution. *IOSR Journal of Applied Chemistry* (IOSR-JAC) e-ISSN: 2278-5736.Volume 7, Issue 7 Ver. III. (July. 2014), www.iosrjournals.org, pp 60-78.

Bashir A. D.; A. Taher; A. Wani and M. Farooqui. (2013). Isotherms and thermodynamic studies on adsorption of copper on powder of shed pods of *Acacia nilotica*, *Journal of Environmental Chemistry and Ecotoxicology* Vol. 5(2), pp. 17-20, February 2013, Available online http://www.academicjournals.org/jece, DOI: 10.5897/JECE12.013, ISSN-2141-226X ©2013 Academic Journals.

Benakashani, F.; A.R. Allafchian and S.A.H. Jalali. (2016). Biosynthesis of silver nanoparticles using Capparis spinosa L. leaf extract and their antibacterial activity. Elsevier published Karbala *International Journal of Modern Science.* http://www.journals.elsevier.com/karbala-international-journal-of-modern-science/. http://dx.doi.org/10.1016/j.kijoms.2016.08.004, pp 1-8

Berekaa, M.M. (2016). Nanotechnology in Wastewater treatment: influence of Nanomaterials on Microbial Systems. *International Journal of Current Microbiology and Applied Sciences*, Volume 5, Number 1, pp 713 – 726.

Chan, Y. J.; M. F. Chong; C. L. Law and D. G. Hassell. (2009). A review on anaerobic–aerobic treatment of industrial and municipal wastewater. School of Chemical and Environmental Engineering, Faculty of Engineering, The University of Nottingham 1385-8947/$ – see front matter © 2009 *Elsevier B.V.* All rights reserved. doi:10.1016/j.cej.2009.06.041, pp 1-18.

Cheng, Q.; H. Li; Y. Xu; S. Chen; Y. Liao and F. Deng (2017). Study on the adsorption of nitrogen and phosphorus from biogas slurry by NaCl- modified zeolite. *PLOS ONE* 12(5): e0176109. https://doi.org/10.1371/journal.pone.0176109, pp 1-12.

Chun Hui Zhou and John Keeling (2013). Fundamental and applied research on clay minerals: From climate and environment to nanotechnology. *Applied Clay Science* 74 (2013) 3–9. http://dx.doi.org/10.1016/j.clay.2013.02.013.

Daizy, P. (2010). Mangifera Indica leaf-assisted biosynthesis of well-dispersed silver nanoparticles. *Spectrochimica Acta*, Part A 78 (2011) 327–331.

Dhaval Patel and Z.Z.Painter (2017). Batch and Column Study for Treatment of Sugar Industry Effluent by using low-cost Adsorbent. Vol-3 Issue-3 2017 *IJARIIE*-ISSN(O)-2395-4396.

Edema, N. (2012). Effects of Crude Oil Contaminated Water on the Environment. Crude Oil Emulsions- Composition Stability and Characterization, *Erratum*. doi:10.5772/36105, pp 1-12.

Fu, F. and Wang, Q. (2011). Removal of heavy metal ions from wastewaters: A review *Journal of Environmental Management*, 92, pp 407-418. doi:10.1016/j.jenvman.2010.11.011.

Galadima, A. and Garba Z. N. (2012). Heavy metals pollution in Nigeria: causes and consequences. *Elixir Pollution*, 45, 7917-7922. Retrieved from www.elixirjournal.org.

Getie S.; A. Belay; R.A. Chandra and Z. Belay. (2017b). Synthesis and Characterizations of Zinc Oxide Nanoparticles for Antibacterial Applications. *J Nanomedic Nanotechnol* 2017, S8. DOI: 10.4172/2157-7439.S8-004, pp 1-8.

Grégorio, C. and Eric L. (2019). Advantages and disadvantages of techniques used for wastewater treatment. Environmental Chemistry Letters, Springer Verlag, 2019, 17 (1), 10.1007/s10311-018-0785-9. hal-02082890, pp.145-155

Haijiao Lu; Jingkang Wang; Marco Stoller; Ting Wang; Ying Bao and Hongxun Hao. (2016). An Overview

of Nanomaterials for Water and Wastewater Treatment. *Review Article.* Hindawi Publishing Corporation Advances in Materials Science and Engineering Volume 2016, Article ID 4964828, http://dx.doi.org/10.1155/2016/4964828, page 1-10.

Haritha M.; V. Meena; C.C. Seema and R.B. Srinivasa. (2011). Synthesis and Characterization of Zinc Oxide Nanoparticles and Its Antimicrobial Activity against Bacillus Subtilis and Escherichia Coli. *Rasayan J.Chem*, Vol.4, No.1 (2011), ISSN: 0974-1496 CODEN: RJCABP, pp 217-222.

Ikhazuangbe P.M.O.; F.I. Kamen; S.O. Opebiyi; M.S. Nwakaudu and O.E. Onyelucheya. (2017). Equilibrium Isotherm, Kinetic and Thermodynamic Studies of the Adsorption of Erythrosine Dye onto Activated Carbon from Coconut Fibre. *International Journal of Advanced Engineering Research and Science (IJAERS) [Vol-4,* Issue-5, May- 2017, https://dx.doi.org/10.22161/ijaers.4.5.9 ISSN: 2349-6495(P) | 2456-1908(O), www.ijaers.com.

Kuranga, I.A.; A.B. Alafara; F. Halimah; A.M. Fausat; O.B. Mercy and B.C. Tripathy. (2018). Production and Characterization of Water Treatment Coagulant from locally sourced Kaolin Clays. *J. Appl. Sci. Environ. Manage*. January, Vol. 22 (1). DOI: https://dx.doi.org/10.4314/jasem.v22i1.19, pp 103-109.

Lo Y.; C. A. Dooyema; A. Neri; J. Durant; T. Jefferies; M.A. Medina; I. Ravello; D. Thoroughman; I. Davis; R.S. Dankoli; M.Y. Samson; L. M.Ibrahim; O. Okechukwu; U. Tsafe; A. H. Dama, and Brown M. J. (2010). Childhood Lead Poisoning Associated with Gold Ore Processing: A Village-Level Investigation—Zamfara State, Nigeria, *Environmental Health Perspectives*, 120:1450-1455. doi:10.1289/ehp.1104793.

Maity, J.; P. Sukanta; M. Sourav and M. Ratul. (2018). Synthesis and Characterization of ZnO Nanoparticles using Moringa Oleifera Leaf Extract: Investigation of Photocatalytic and Antibacterial Activity. *Int. J. Nanosci. Nanotechnol*., Vol. 14, No. 2, June. 2018, pp. 111-119.

Manokari, M. and Mahipal, S.S. (2016). Zinc oxide nanoparticles synthesis from *Moringa oleifera* Lam - Extracts and their characterization. *WSN* 55 (2016) EISSN 2392-2192, pp 252-262.

Ming H.; Z. Shujuan; P. Bingcai; Z. Weiming; L. Lu and Z. Quanxing. (2012). Heavy metal removal from water/wastewater by nanosized metal oxides: A review. *Journal of Hazardous Materials* 211– 212 (2012), pp 317–331.

Mohd, S.Y.; A.K. Mohamad; A.A. Hamidi and A.O. Christopher. (2013). Recent Developments of Textile Wastewater Treatment by Adsorption Process: A Review. *International Journal of Scientific Research in Knowledge (IJSRK)*, 1(4), 2013 Available online at http://www.ijsrpub.com/ijsrk ISSN: 2322-4541. pp. 60-73.

Murray H. H. (2000). Traditional and new applications for kaolin, smectite, and palygorskite: a general overview. *Applied Clay Science* 17 _2000. 207–221.

NBS. (2017). State Disaggregated Mining and Quarrying Data. *National Bureau of Statistics*, Nigeria.

NESREA (2011). National Environmental Standards Regulations and Enforcement Agency. *National Environmental (Surface and Groundwater Control) Regulations, 2011*. Printed and published by the Federal Government Printer, LAgs, Nigeria. FGP71/72011/400 (OL,46), pp 1-6.

Njagi E.C.; H. Hui; Lisa Stafford; G. Homer; M.G. Hugo; B.C. John; E.H. George and L.S. Steven. (2010). Biosynthesis of Iron and Silver Nanoparticles at Room Temperature Using Aqueous Sorghum Bran Extracts. DOI: 10.1021/la103190n Published on Web 12/06/2010 *Langmuir* 2011, 27(1), pp 264–271.

NWQRL (2020). Atlas of Rivers and Open Waterbodies Monitoring Activities, National Water Quality Reference Laboratories (NWQRL), Department of Water Quality Control and Sanitation, *Federal Ministry of Water Resources*, Abuja.

Okereke, J. N.; O. I. Ogidi and K. O. Obasi. (2016). Environmental and Health Impact of Industrial Wastewater Effluents in Nigeria - A Review, *Int. J. Adv. Res. Biol. Sci.* (2016). 3(6): http://s-o-i.org/1.15/ijarbs-2016-3-6-8, pp 55-67.

Rajasulochana, P. and Preethy V. (2016). Comparison on efficiency of various techniques in treatment of waste and sewage water – A comprehensive review, http://dx.doi.org/10.1016/j.reffit.2016.09.004, *Resource-Efficient Technologies*, pp 175–184.

Rakhi M.S.; B.G. Suresh and M. Premalatha. (2016). Applications of Nanotechnology in Wastewater treatment: A Review. *Imperial Journal of Interdisciplinary Research (IJIR)* Vol-2, Issue-11, 2016 ISSN: 2454-1362, http://www.onlinejournal.in.

Ralf, K.i; V. Andreas; S. Brian; Z. Steffen; H. Harald; B. Michael and S. Hansruedi. (2011). Behaviour of Metallic Silver Nanoparticles in a Pilot Wastewater Treatment Plant. ACS publications, pubs.acs.org/est. dx.doi.org/10.1021/es1041892 *Environ. Sci. Technol*. 2011, 45, pp 3902–3908.

RMRDC. (2018). National Distribution of Raw Materials – Niger State, Raw Material Research and Development Council.

Roadmap (2022). Nigeria Roadmap for Water Quality, *Federal Ministry of Water Resources*, Draft Copy, 2022.

Rui M.; L. Clément; D.J. Jonathan; M.U. Jason; Mark Durenkamp; Ben Martin; Bruce Jefferson and Gregory Victor Lowry. (2013). Fate of zinc oxide and silver nanoparticles in a pilot wastewater treatment plant and in processed biosolids. *Environ. Sci. Technol*. Downloaded from http://pubs.acs.org.

Sachin K.; K.P. Achyut and R. K. Singh. (2013). Preparation and Characterization of Acids and Alkali Treated Kaolin Clay. *Bulletin of Chemical Reaction Engineering and Catalysis*, 8 (1), 2013, http://bcrec.undip.ac.id, pp 61 – 69.

Saikia N.J.; D.J. Bharali; P. Sengupta; D. Bordoloi; R.I. Goswamee; P.C. Saikia and P.C. Borthakur. (2003). Characterization, beneficiation and utilization of a kaolinite clay from Assam, India. *Applied Clay Science* 24 (2003) 93–103. doi:10.1016/S0169-1317(03)00151-0

Shittu K.O and Ikebana, O.(2017). Purification of simulated waste water using green synthesized silver nanoparticles of *Piliostigma Thonningii* aqueous leave extract. *Adv. Nat. Sci.: Nanosci. Nanotechnol*, https://doi.org/10.1088/2043-6254/aa8536.

Sierra, M.J; P.Adriana; Herrera and Karina A.O. (2018). Synthesis of Zinc Oxide Nanoparticles from Mango and Soursop Leaf Extracts. *Contemporary Engineering Sciences*, Vol. 11, 2018, no. 8, https://doi.org/10.12988/ces.2018.8228, pp 395 – 403

Stoyanova A.; H. Hitkova; A. Bachvarova-Nedelcheva; R. Iordanova N.I. and Sredkova, M (2013). *Journal of Chemical Technology and Metallurgy*, 48, 2, pp 154-161.

Sukdeb Pal; Yu Kyung Tak and Joon Myong Song (2007). Does the Antibacterial Activity of Silver Nanoparticles Depend on the Shape of the Nanoparticle? A Study of the Gram-Negative Bacterium Escherichia coli. *Applied and Environmental Microbiology*, Mar. 2007, Vol. 73, No. 6 0099-2240/07/$08.00_0 doi:10.1128/AEM.02218-06, pp 1712–1720.

Sulekha, M.S. (2016). Nanotechnology for Wastewater Treatment. *International Journal of Chemical Studies*; 4(2), Pp 22 – 24.

Syafiqa A.; O. Norzila; A.H.A Wahid; S.K Faisal; A.B. Norshila; T. Muhammad and S.S. Eddy. (2021). A Review on Adsorption of Heavy Metals from Wood-Industrial Wastewater by Oil Palm Waste. *Journal of Ecological Engineering* 2021, 22(3), https://doi.org/10.12911/22998993/132854 ISSN 2299-8993, License CC-BY 4.0, pp 249–265.

Thabet, M.; A.M. Tolaymat; B. El; G. Ash; G. Kirk; T.P. Scheckel and M.S. Luxton. (2010). An evidence-based environmental perspective of manufactured silver nanoparticle in syntheses and applications: A systematic review and critical appraisal of peer-reviewed scientific papers. Published by *Elsevier B.V.*, doi:10.1016/j.scitotenv.2009.11.003 Science of the Total Environment 408 (2010) pp 999–1006.

Thirunavukkarasu, R.; S. Archana; B. Sharmila; Janarthanan and J. Chandrasekaran. (2016). Preparation and Characterization of Zno Nanoparticles Using *Moringa Oleifera* Extract by Green Synthesis Method. *Asian Journal of Phytomedicine and Clinical Research*, www.uptodateresearchpublication.com.

Vikas, S. and Akhilesh S. (2013). Nanotechnology: An Emerging Future Trend in Wastewater Treatment with its Innovative Products and Processes. *International Journal of enhanced Research in Science Technology and Engineering.* Vol.2 Issue 1, Dec – 2013, ISSN No: 2319 – 7463. pp 1 – 6.

Wilson A.M. (2017). Crystallization of NBA-ZSM-5 from kaolin. Doctoral thesis, Department of Civil, Environmental and Natural Resources Engineering Division of Chemical Engineering, *Luleå University of Technology*.

Worldometer (2023). Nigeria Population, https://www.worldometers.info/world-population/nigeria-population/, access February, 2023.

Yahaya S.; S.J. Suzi; A.B. Nur and D.A. Ajiya. (2017). Chemical Composition and Particle Size Analysis of Kaolin, *Path of Science*. Vol. 3, No 10 ISSN 2413-9009. DOI: 10.22178/pos.27-1.

Yang Z.; C. Yongsheng; W. Paul; H. Kiril and C.C. John. (2008). Stability of commercial metal oxide nanoparticles in water. 42 (2008), doi:10.1016/j.watres.2007.11.036, pp 2204 – 2212.

Ying C.; D. Hao and S. Sijia. (2017). Preparation and Characterization of ZnO Nanoparticles Supported on Amorphous SiO2. Nanomaterials 7, 217; doi:10.3390/nano7080217 www.mdpi.com/journal/nanomaterials.